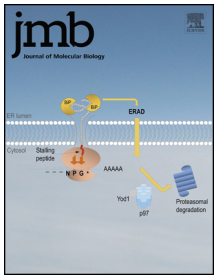

Molecular Mechanism of Spontaneous Nucleosome Unraveling

David Winogradoff[1,2] **and Aleksei Aksimentiev**[1,2,3]

*1 - **Center for the Physics of Living Cells,** University of Illinois at Urbana–Champaign, Urbana, IL 61801, USA*
*2 - **Department of Physics,** University of Illinois at Urbana–Champaign, Urbana, IL 61801, USA*
*3 - **Beckman Institute for Advanced Science and Technology,** University of Illinois at Urbana–Champaign, Urbana, IL 61801, USA*

***Correspondence to Aleksei Aksimentiev:** Center for the Physics of Living Cells, University of Illinois at Urbana–Champaign, Urbana, IL 61801, USA. aksiment@illinois.edu*
https://doi.org/10.1016/j.jmb.2018.11.013
Edited by Anna Panchenko

Abstract

Meters of DNA wrap around histone proteins to form nucleosomes and fit inside the micron-diameter nucleus. For the genetic information encoded in the DNA to become available for transcription, replication, and repair, the DNA–histone assembly must be disrupted. Experiment has indicated that the outer stretches of nucleosomal DNA "breathe" by spontaneously detaching from and reattaching to the histone core. Here, we report direct observation of spontaneous DNA breathing in atomistic molecular dynamics simulations, detailing a microscopic mechanism of the DNA breathing process. According to our simulations, the outer stretches of nucleosomal DNA detach in discrete steps involving 5 or 10 base pairs, with the detachment process being orchestrated by the motion of several conserved histone residues. The inner stretches of nucleosomal DNA are found to be more stably associated with the histone core by more abundant nonspecific DNA–protein contacts, providing a microscopic interpretation of nucleosome unraveling experiments. The CG content of nucleosomal DNA is found to anticorrelate with the extent of unwrapping, supporting the possibility that AT-rich segments may signal the start of transcription by forming less stable nucleosomes.

Introduction

Eukaryotic DNA wraps around histone proteins to form arrays of nucleosomes, ultimately organizing into chromosomes. For DNA to become available for template-directed processes—transcription in particular—nucleosomes must be disrupted or displaced [1]. The mechanical stability of a nucleosome is determined by the strength of histone–DNA contacts and the mechanical properties of the nucleosomal DNA [2,3]. Specifically, *in vitro* experiments [4–7], bioinformatics analysis [8], and structural studies [9] have identified CG content [5,8] the placement of TA dinucleotides [5,7], and the presence of CA=TG steps [9] as important determinants of nucleosome stability. Experimental studies have also shown that the outer stretches of DNA can spontaneously unwrap and rewrap from the histone core in a process known as "DNA breathing" [6,7,10–17]. Recent *in vitro* single-molecule studies revealed that nucleosomes unwrap asymmetrically under force, and that the preferred direction of unwrapping depends on the DNA sequence [7].

It is also important to consider what is not yet fully known concerning nucleosome occupancy and stability. Experimental and bioinformatics studies indicate that DNA sequences with greater CG content form more stable nucleosomes. However, nucleosomes have been shown to be depleted in so-called "CpG islands," regions of elevated CG content and reduced methylation [18–20]. Furthermore, several specific DNA sequence motifs have also been proposed to be important, including "TA" dinucleotides [4,7,21], poly-A tracts [22], and "TATA" box regions [23]. The very mechanism of DNA unwrapping from a histone core is also under debate. Several different modes of nucleosome motion have been observed or proposed, including "DNA breathing" described above, the splitting of histone dimers of H2A and H2B from the histone core, which could accompany DNA

unwrapping [14,24,25], the propagation of a loop [26] or twist defect [27], and the "gaping" between superhelical turns of DNA without unwrapping [28]. It is also possible that nucleosome repositioning *in vivo* may involve several different mechanisms.

Computational studies play an important role in examining nucleosome structure and dynamics, providing insight into microscopic details not readily accessible to experiment. Previous coarse-grained [29–34] and all-atom [35–44] molecular dynamics (MD) simulations have investigated the dynamics of nucleosomes and chromatin. Coarse-grained studies have primarily been used to examine DNA positioning and superhelical sliding [45,46], or the free energy associated with nucleosomal unwrapping [30–32], without commenting on how spontaneous detachment occurs at the molecular level. Previous all-atom MD simulations have characterized nucleosomal DNA's primary modes of motion [35], discovered that the nucleosome behaves like a sponge absorbing water and ions [36], unwrapped nucleosomal DNA by force [38,47], uncovered transient elements of structure in histone tails [37,41,43,48–50], and found that histone variation may lead to enhanced flexibility [39,40,42,51]. The spontaneous detachment of about one turn of DNA from a histone core has been observed in all-atom simulations [39,40,43], but those reports did not to attempt to describe the underlying mechanism. Multiscale MD studies have combined all-atom and coarse-grained simulations [41,52,53] to form hypotheses on the potential role of histone tails in short-length [i.e., under 10 base pairs (bp)] nucleosomal DNA detachment [53] and in the mediation of nucleosome–nucleosome interactions [41]. Studies that use theory, or a combination of theory and simulation, have taken a more mathematical approach to investigating the possible effects of DNA sequence on nucleosome stability [54] and DNA flexibility [55]. Large-scale, all-atom simulations were also used to investigate how nucleic acids bend around nanoparticles designed to mimic histones [56]. Overall, a mechanistic account of spontaneous nucleosomal DNA detachment in atomistic detail has remained largely elusive.

Here, we report the molecular mechanism of spontaneous unraveling of nucleosome core particles observed in all-atom MD simulations. Our study examined nucleosomal DNA breathing at multiple ionic conditions and for several DNA sequences. We identified a stepwise mechanism, involving a set of specific histone residues, that leads to the detachment of outer turns of nucleosomal DNA by observing many spontaneous detachment events in all-atom detail. Through another set of simulations, where DNA detachment was induced through partial rupture of the specific contacts, we confirmed the proposed mechanism and further probed the effects of DNA sequence. A mechanistic account of nucleosome unwrapping and the effects of DNA sequence therein are key to understanding fundamental biological processes, including transcription, replication, and repair.

Results and Discussion

Spontaneous and reversible nucleosomal unwrapping

Figure 1a illustrates a typical simulation system considered in this work: an all-atom model of a nucleosome (PDB ID: 3LZ0 [57]) submerged in an electrolyte solution. Several simulation systems were constructed featuring a 601L nucleosome, differing by the electrolyte conditions: 0.15 M NaCl, 1.0 M $MgCl_2$, and 3.0 M NaCl. The protein core of each model contained residues 16–118 for both copies of H2A, 29–121 for both copies of H2B, 39–134 for both copies of H3, and 25–102 for both copies of H4. The disordered N- and C-terminal tails of the core histones were not included in the nucleosome models. Based on the results of several experimental studies [58,59], we anticipate that the removal of histone tails has accelerated the rate of spontaneous DNA unwrapping. See Materials and Methods for further details on the simulation protocol.

For each nucleosome system considered, three independent replica simulations were performed separately, including minimization and structural relaxation, followed by approximately 0.35 μs of free equilibration at room temperature and standard pressure conditions. Initial velocities for replica simulations were generated using unique random seeds. The pairwise RMSD values at the beginning of free equilibration simulations ranged from 2.3 to 3.5 Å across all replica simulations (see Supplementary Fig. S1). In one of three replica simulations carried out for each 1.0 M $MgCl_2$ and 3.0 M NaCl electrolyte condition, the nucleosomal DNA was observed to detach spontaneously within the first 0.35 μs. These two simulations were extended to 2 μs using DESRES Anton2 special purpose supercomputer [60]. Although no spontaneous DNA detachment was observed within the first 0.35 μs of the three 0.15 M NaCl simulations, one replica simulation was extended to 2 μs for comparison with the 1.0 M $MgCl_2$ and 3.0 M NaCl systems.

In general agreement with salt-dissociation experiments [21,61,62], the structural stability of a nucleosome was found to depend on the electrolyte conditions used in an MD simulation. At physiological electrolyte concentration (0.150 M NaCl), the Widom 601L DNA remained stably bound to the histone core over the entire 2 μs simulation (Fig. 1b and Supplementary Movie 1). Such high integrity of

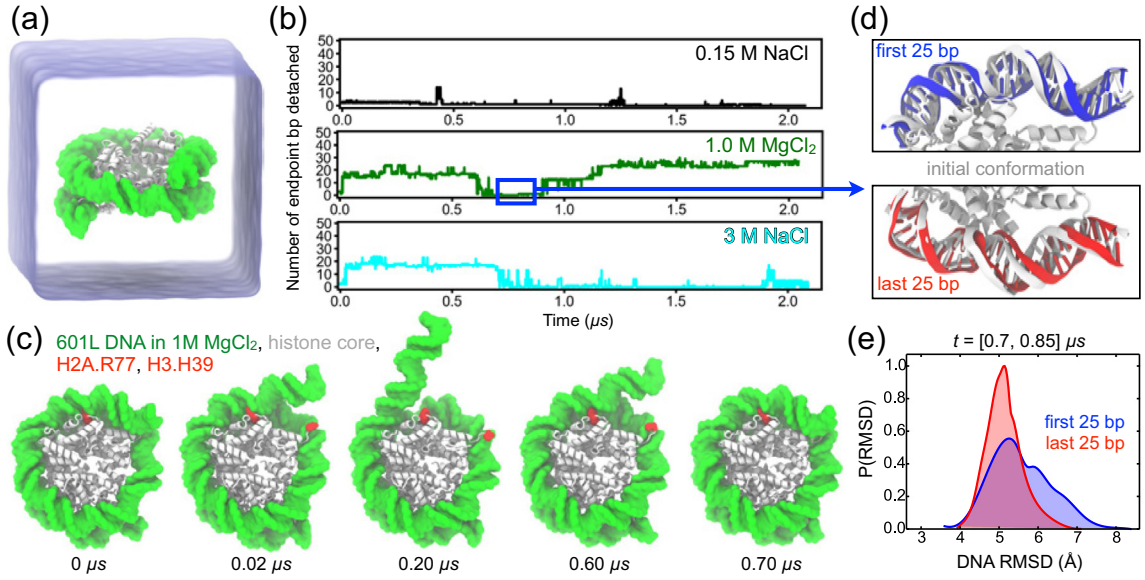

Fig. 1. All-atom MD simulation of DNA breathing. (a) Simulation setup: a nucleosome particle composed of a histone core (white) and a 145-bp fragment of DNA (green) is surrounded by electrolyte solution (semi-transparent blue). (b) The number of endpoint bp detached from the histone core as a function of time in the simulations of the Widom 601L nucleosome performed in 0.15 M NaCl (top), 1.0 M $MgCl_2$ (middle), and 3.0 M NaCl (bottom). The number of endpoint bp detached was determined by finding all DNA–histone contacts, defining a contact as a pair of non-hydrogen atoms of the protein and DNA located within 4.5 Å of each other, and identifying the contact-forming DNA bps closest to the entry and exit termini, the terminal contact bps. The total number of bp detached was calculated as the total number of bps in the nucleosomal DNA (i.e., 145) minus the number of bps located between the terminal contact bps. (c) Snapshots illustrating spontaneous unbinding and rebinding of nucleosomal DNA from and to the histone core observed in 1 M $MgCl_2$ solution. Starting from a fully bound state (0 μs), two DNA–histone contacts from the entry side break (0.02 μs, 0.20 μs) and later reform (0.60 μs, 0.70 μs). H2A Arg77 and H3 His39 are highlighted in red. (d) Reversibility of DNA detachment. Top and bottom panels illustrate the microscopic configurations of the two terminal fragments of DNA (first and last 25 bp, respectively) at the beginning (white) and after 0.8 μs (red and blue) of the MD simulation performed in 1.0 M $MgCl_2$. The DNA fragment featured in the top panel unbinds from and rebinds to the histone core within the first 0.7 μs of the simulation. (e) Normalized distributions of the DNA fragments' RMSD values for the [0.70, 0.85] μs segment of the 1.0 M $MgCl_2$ trajectory. The RMSD values were computed with respect to the starting conformations using coordinates of all non-hydrogen DNA atoms, after alignment of the histone core backbone atoms.

the nucleosome structure is consistent with the experimentally characterized timescale of 250 ms for the outer stretch of nucleosomal DNA to unwrap from a histone core at physiological conditions [63]. In a simulation carried out at high ionic strength electrolyte (1.0 M $MgCl_2$), the outer turns of the 601L nucleosomal DNA unwrapped spontaneously from the histone core in a stepwise fashion (Fig. 1b); 601L DNA also became detached in another condition of high ionic strength (3.0 M NaCl). Figure 1c and Supplementary Movie 2 illustrate the simulated DNA unbinding process in 1 M $MgCl_2$, and Supplementary Movie 3 depicts a similar process in 3 M NaCl. Conditions of high ionic strength apparently reduce the electrostatic attraction between the negatively charged DNA and the positively charged histone core, thereby increasing the likelihood of DNA unwrapping. Three-dimensional density maps of Mg^{2+} and Na^+ (Supplementary Fig. S2a and b) indicate that both ion species can enter both minor and major grooves of the nucleosomal DNA, and that Na^+ ions cover the DNA's surface more evenly than Mg^{2+}, matching the results of a previous study [64]. Note that, because the simulation time scale does not exceed single digit microseconds, we do not expect to observe complete unraveling of nucleosomal DNA, as observed in experiment performed at a much longer time scale [21,62]. Our simulations, thus, probe recovery of the system to equilibrium following the quench of ionic conditions, revealing the details of the nucleosome unraveling process.

To estimate the rate of unwrapping conditioned by the DNA elasticity alone, we simulated the Widom 601L DNA in the absence of the histone core starting from the conformation the DNA adopts in an intact nucleosome. The DNA was observed to unravel completely from its starting conformation within 300 ns of the simulation (see Supplementary Movie 4).

The simulated spontaneous unraveling of the nucleosomal particle was found to be reversible. In 3.0 M NaCl, about 13 bp of 601L DNA became

detached around 0.03 μs, and then reattached to the histone core by 0.9 μs (see Fig. 1b and Supplementary Movie 4). In the simulation carried out at 1.0 M $MgCl_2$, the first 25 bp of the nucleosomal DNA underwent two major detachment transitions, at 0.02 and 0.20 μs, but bound back to the histone core in two separate steps, at 0.60 and 0.70 μs (Fig. 1b and c). Furthermore, the DNA appears to bind back to the histone core in a conformation that is statistically indistinguishable from its initial state. To illustrate this point, we show in Fig. 1d the conformations of the terminal 25 bp of the nucleosomal DNA at the beginning of the simulation (0 μs) and after undergoing a reversible unbinding transition (0.7 μs). The overlay of the two conformations visually appears indistinguishable for the entry (first 25 bp) and exit (last 25 bp) termini of the nucleosomal DNA, although only the entry fragment underwent reversible unraveling while the exit fragment remained bound to the histone core. The distributions of the DNA fragments' RMSD values with respect to their starting positions (both with primary peaks between 5.0 and 5.5 Å; Fig. 1e) illustrate the dynamic nature of these segments and the statistical similarity of their conformations upon reversible unbinding. The difference in the RMSD distributions arises from greater fluctuations of the initial 10 bp of the first 25 bp, compared to the final 10 bp of last 25 bp (Supplementary Fig. S3). Such spontaneous, reversible unwrapping of DNA was previously observed in experiment [6,65] and was described as "DNA breathing."

The effects of DNA sequence on nucleosome breathing

To examine the effects of the nucleotide sequence on DNA breathing, we repeated the simulations of the nucleosomal system at 1 M $MgCl_2$ for the three additional variants of the nucleosomal DNA sequence: poly-AT (i.e., ATAT…; 0% CG), 5S mRNA gene (43% CG) [66], and poly-GC (i.e., GCGC…; 100% CG), which are known to form nucleosomes *in vitro* [66–68]. The nucleotide bases of the 601 DNA resolved in the X-ray structure were changed according to the target sequence (listed in Supplementary Table S1) while keeping the same conformation of the DNA backbone. Materials and Methods and Table S2 provide a detailed description of the structure building and simulation protocols. As done for 601L, three replica simulations were performed for the additional sequences in 1 M $MgCl_2$ for 0.35 μs. One replica of poly-AT and one of 5S gene underwent spontaneous detachment in that time period and were extended to 2 μs. No replicas of poly-GC exhibited detachment within 0.35 μs, and one was extended to 2 μs for the sake of comparison.

Among the four systems (601L, poly-AT, 5S and poly-CG), the poly-AT system was found to be the most dynamic (Fig. 2a). Within the first ~0.8 μs of the simulation, about 45 bp detached from the histone core in four unbinding events occurring at both DNA termini, followed by the subsequent rebinding of about 20 bp; Supplementary Movie 5 illustrates this MD trajectory. The outcome of the 5S nucleosome simulation was similar to that of 601L: 25 bp ultimately became unwrapped within 2 μs (Fig. 2a and Supplementary Movie 6), which can be attributed to the similarity in CG content of their DNA sequences. On the other hand, none of the poly-GC bp unwrapped from the histone core (Fig. 2a and Supplementary Movie 7), despite considerable structural fluctuations. Thus, the extent of simulated DNA unraveling (Fig. 2b) appears to be correlated with the CG content: the poly-AT (0% CG) nucleosome unravels the most, the 5S (43% CG) and 601L (57% CG) nucleosomes display intermediate unraveling, and the poly-GC (100% CG) one does not unravel. Unlike the other DNA sequences considered, 5S is asymmetric: the 5′ side contains ~38% CG, and the 3′ side contains ~50% CG. As shown in Supplementary Fig. S4a, 5S DNA spontaneously unwraps from the 5′ side, the side smaller in CG content. This result is consistent with our overall finding that DNA sequences lower in CG content are less stably attached to a histone core. We also note that more 5S DNA unbinding events would need to be observed to definitively conclude that spontaneous unwrapping primarily occurs from one side.

The results of our MD simulations suggest that a DNA molecule with greater CG content may form a more stable nucleosome, in agreement with the aforementioned bioinformatics analysis [4,5,8]. Our results are also consistent with a recent computational study that found nucleosomes to slide more slowly along poly-GC DNA, and more rapidly along poly-AT [69]. A set of independent simulations of 45 bp DNA fragments in 0.15 M NaCl and 1.0 M $MgCl_2$ showed a statistically insignificant dependence of the dynamic persistence length [55] on the electrolyte conditions (see Supplementary Note 1 and Fig. S5), consistent with experimental studies that found only a small change in DNA's persistence length when increasing from moderate to high salt concentrations [70,71]. The possible implications of our results are also in agreement with a single-molecule experimental study that found a difference in the CG content of the left and right halves of nucleosomal DNA to determine, in part, the preferred direction of asymmetric unwrapping under tension [7]. To add more statistical weight to these results of spontaneous unbinding, we revisit the effects of DNA sequence below in computational assays where detachment is induced.

The stepwise mechanism of nucleosomal DNA unraveling

Close inspection of the MD trajectories reveals that a DNA–histone unbinding event is a two-step

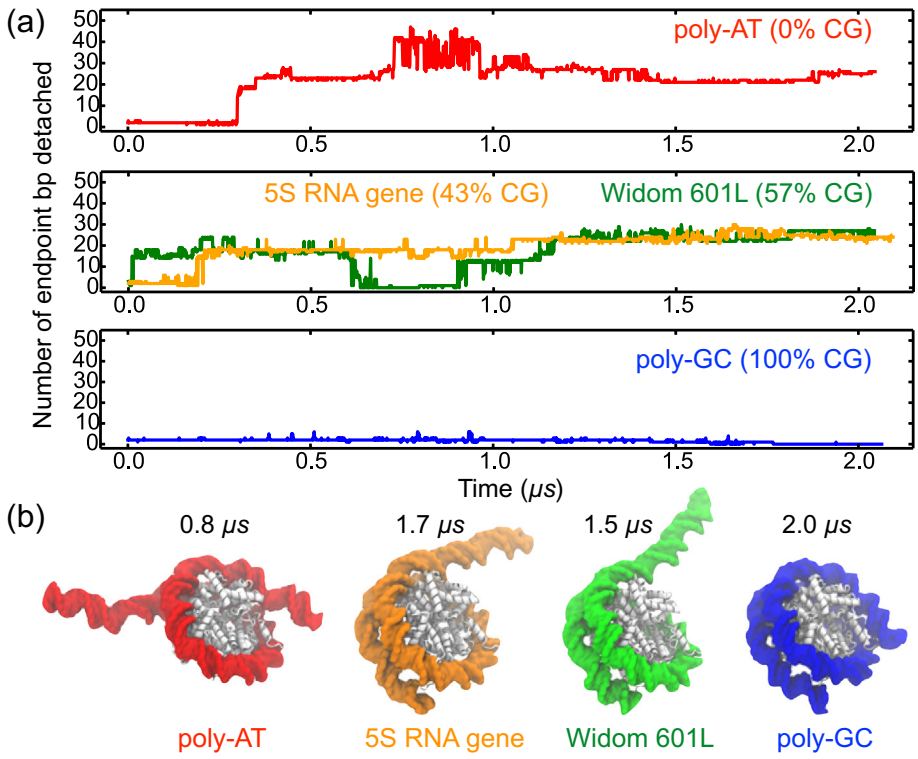

Fig. 2. The effect of CG content on spontaneous unwrapping of a nucleosome. (a) The number of endpoint bp detached from the histone core as a function of simulation time for nucleosomes containing DNA of poly-AT (0% CG), 5S RNA gene (43% CG), Widom 601L (57% CG), and poly-CG (100% CG) nucleotide sequences. The 601L sequence trace is the same as in Fig. 1b. All nucleosome variants were simulated in 1.0 M $MgCl_2$ electrolyte. (b) Representative conformations of the nucleosome systems corresponding to the states characterized by the maximum detachment of the nucleosomal DNA.

process, controlled by the conformation of several histone residues. These residues—H3 His39, H3 Arg40, H3 Arg49, H2A Arg30, H2A Arg77—are all conserved for at least 84% of species that contained a functional equivalent of human histone proteins H3.1 and H2A.1 [72]. Figure 3a and b depicts a typical DNA–histone unbinding event, illustrating the distinct steps of the process. Initially, DNA binding to the histone core is stabilized by a charged side chain that is inserted into the minor groove of DNA and simultaneously forms salt bridges with two phosphate groups from different DNA strands (Fig. 3b i). The detachment begins after one of the salt bridges breaks, leaving the charged side chain interacting only with one of the DNA strands (Fig. 3b ii). After the second DNA–histone salt bridge breaks, one turn of DNA becomes detached from the histone core (Fig. 3b iii). For the example highlighted, the entire process leads to the detachment of about 10 bp, with the intermediate state (from ~0.18 to 0.20 μs) corresponding to the release of 5 bp. Supplementary Fig. S6 and Table S2 characterize the process of DNA unbinding for each major spontaneous detachment observed, showing that an intermediate partially bound state occurred in each detachment event although the number of bp released during the intermediate step varied.

In 7 out of 11 unbinding events, 4 or 5 bps were released at the intermediate step, whereas no bps were released in the other four unbinding events (Supplementary Table S2). This observation is consistent with the results of a recent experimental study that found DNA to unwrap from the histone core predominantly in 10-bp steps that sometimes included an intermediate 5-bp step [73]. The proposed mechanism provides an explanation of why 5- or 10-bp unwrapping steps could occur. Our simulations revealed that the detachment of one turn of a DNA helix requires the sequential breaking of two salt bridges formed with the same histone residue. Because the nucleosomal DNA is in an over-twisted state, the phosphates that form these two interactions with the same histone residue are spaced about 5 bp apart on the opposite strands of the DNA duplex. Depending on which of the two salt bridges breaks first, the unwrapping can occur in two 5-bp steps or one 10-bp step. The rebinding of nucleosomal DNA to the histone core may follow a slightly different mechanism where a histone side chain slides along the DNA backbone before reinserting

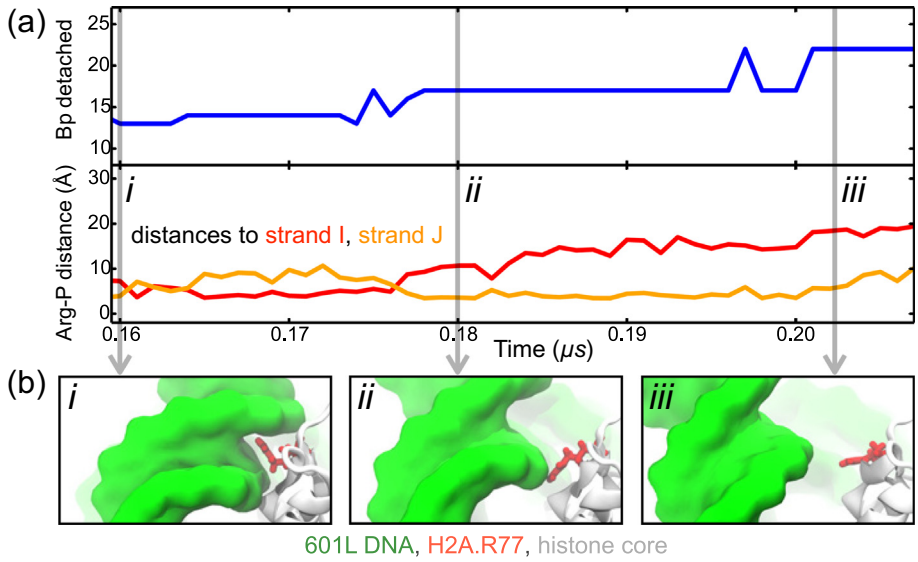

Fig. 3. Stepwise unraveling of nucleosomal DNA. (a) The number of endpoint bp detached (top) and the distance from the guanidinium group of H2A Arg77 to the nearest phosphorus atom of the I (red) and J (orange) strands of nucleosomal DNA (bottom) *versus* simulation time. These data are derived from an MD simulation of the 601L nucleosome in 1 M $MgCl_2$. (b) Snapshots illustrating the steps of DNA–histone unbinding. Nucleosomal DNA (green) transitions from being tightly bound to the histone core (white) by a charged residue (red) to only being partially bound to the core (*i* → *ii*); then DNA detaches completely from the core (*ii* → *iii*). A similar pattern of unbinding was observed for all detachment events (see Supplementary Table S2 and Fig. S6).

into the minor groove (see Supplementary Movie 2). As previously suggested by Kulić and Schiessel [74], we have encountered five instances of a 1-bp shift in the interaction between DNA phosphates and key histone residues out of 16 observed unwrapping or rewrapping events (Supplementary Fig. S7). Therefore, in our simulations, we have observed a combination of spontaneous nucleosome unwrapping and rewrapping, and the formation of twist defects that arise from a 1-bp shift in DNA–histone interaction.

To test the proposed mechanism of nucleosome breathing and its dependence on DNA sequence, we performed three independent replica simulations each of poly-AT, 5S gene, 601L, and poly-GC nucleosomes in 1.0 M $MgCl_2$ where unwrapping was induced by partially rupturing essential DNA–histone contacts. The side chains of 10 key histone residues were moved and held, away from the three outermost locations of histone–DNA minor groove contacts at either termini of nucleosomal DNA, six such locations in total. Figure 4a illustrates the extent of the initial forced side chain motion for 1 of the 10 residues forming the DNA–histone contacts; Supplementary Methods 1, Fig. S8, and Table S3 describe the details of the simulation protocol.

The partial rupture of the essential DNA–histone contacts was found to produce rapid unbinding of the DNA terminal fragments (Fig. 4b and Supplementary Movie 8). Unwrapping occurred for all DNA sequences considered within 0.2 μs, one-tenth of the timescale explored for spontaneous unraveling. The average number of bps detached at the end of these simulations is shown graphically in Fig. 4c. Poly-AT, containing 0% CG, had an average of 28.7 ± 4.1 endpoint bp detached after about 0.21 μs, the least CG and most bps detached on average. Over the same time period, an average of 26.0 ± 3.3 bp of 5S gene (43% CG) and 24.7 ± 9.9 bp of 601L (57% CG) became detached. Poly-GC, which is 100% CG, had an average of 16.7 ± 1.7 bp detached, the fewest of all sequences considered. The results of accelerated unwrapping when holding histone residues away from DNA demonstrate that greater CG content leads to a more stable nucleosome, expanding upon what was observed from simulations of spontaneous unraveling (Fig. 2). Furthermore, keeping the specific histone side chains held away prevented the nucleosomes from rewrapping. Across all systems in which histone–DNA contacts were ruptured, the DNA unraveling did not progress beyond 27 bp from either endpoint.

Central nucleosomal DNA more stably interacts with the histone core

Our results suggest that the outermost three turns of nucleosomal DNA unwrap more easily from the histone core than the inner DNA, implying that the latter is more strongly bound. Depicted in Fig. 5a, a nucleosome featuring only the central 85 bp of Widom 601 DNA (58% CG) was simulated to examine

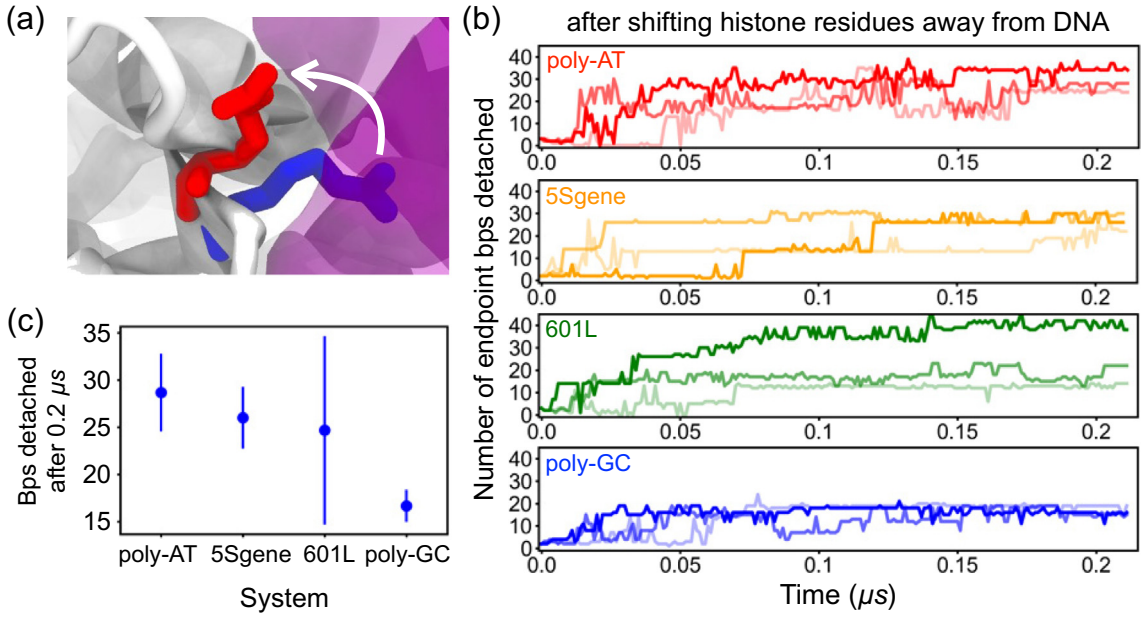

Fig. 4. Test of the nucleosome dissociation mechanism. Specific DNA–histone core contacts were simultaneously broken by forcibly moving the side chains of the contact residues away from the DNA in a 10-ns MD simulation. (a) One of the 10 DNA–histone contact forming residues before (blue) and after (red) the contact rupture; the DNA and histone core are shown as purple and white molecular surfaces, respectively. (b) The number of endpoint bp detached during simulations that followed the forced contact rupture; the histone side chains were kept away from the DNA. Colored labels indicate the nucleosomal DNA sequences. Three independent replicas were run for each system. Simulations were performed in 1.0 M $MgCl_2$ electrolyte. (c) The average number of endpoint bps detached from the histone core after 0.2 μs of holding key histone residues away from the DNA. Error bars represent standard deviations. DNA sequences are ordered from left to right by increasing CG content.

the stability of inner nucleosomal DNA in the absence of outer DNA. Over the first 0.75 μs of simulation, one brief DNA detachment was observed from the entry side, and one brief detachment from the exit side, shown in Fig. 5a and Supplementary Movie 9. For the rest of the time, the DNA remained stably bound to the histone core, with several short-lived partial detachments, indicating that inner DNA unwraps at a slower rate than outer DNA. Contact analysis of our MD trajectories demonstrates that the inner region of the nucleosomal DNA forms more contacts on average with the histone core than the outer region (Fig. 5b and c). Interestingly, the DNA sequence does not affect the average number of contacts for each region (Fig. 5c), indicating that the difference in the unbinding kinetics of the outer regions is caused by DNA mechanics, not DNA–protein contacts. Further analysis indicates that detachment of the outer stretches of DNA from the histone core does not influence the number of contacts that the inner stretches of DNA make with the histone core (Fig. S5). We note also that the number of DNA–histone contacts does indeed change over time throughout the 2-μs production MD simulations (see Supplementary Fig. S9a). In agreement with our observations, larger forces were required to unwrap inner stretches of nucleosomal DNA in single-molecule experiments [7,73].

Interestingly, the DNA in 601L and 5S systems was found to detach spontaneously almost exclusively from one side in 1 M $MgCl_2$ similar to the behavior of the 601L system in 3 M NaCl (Fig. S4a). On the other hand, poly-AT in 1 M $MgCl_2$ is seen to detach from both ends simultaneously (Fig. S4a). After rupturing key histone–DNA contacts, or when considering a nucleosome system with only the central 85 bp of DNA, detachment occurs fairly evenly from both sides (Fig. S4b and c). Thus, our simulations neither confirm nor rule out the possibility that detachment of nucleosomal DNA from opposite sides may be coordinated.

Conclusions

In this study, MD simulations were used to characterize nucleosome unwrapping in atomistic detail, uncovering the effects of ionic conditions (Fig. 1), DNA sequence (Figs. 2 and 4), and DNA position with respect to the pseudo-dyad (Fig. 5). By closely examining many major DNA–histone spontaneous unbinding events (Fig. 3a and b and Supplementary Fig. S6), we recognized a clear two-step mechanism of detachment: (1) periodically placed DNA transitions from being fully bound to a specific positively charged residue of the histone core to being only

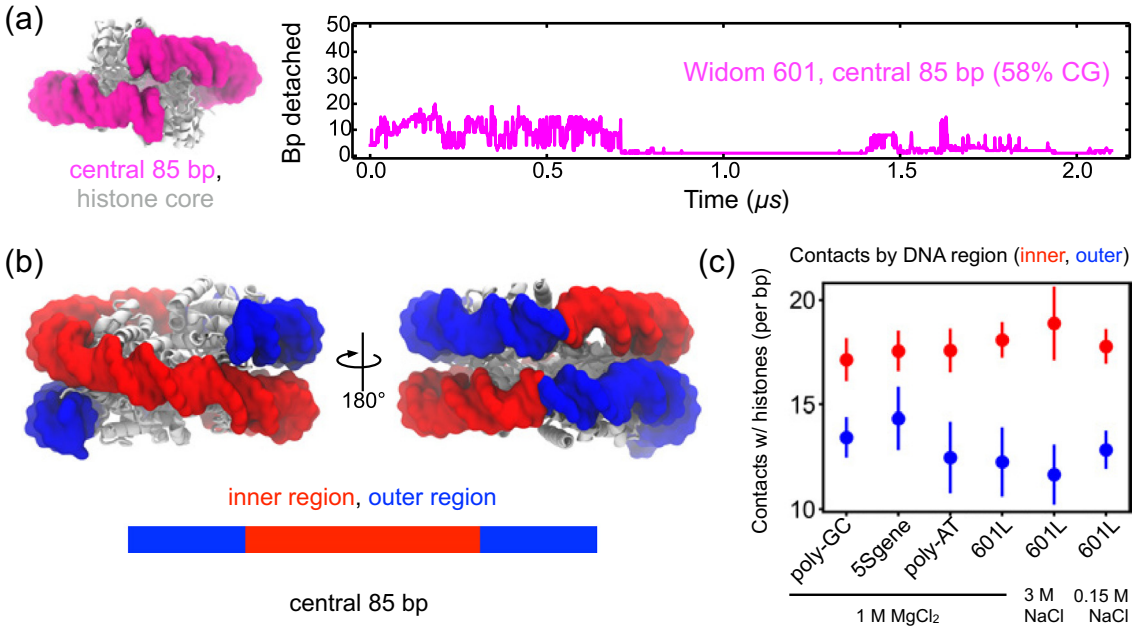

Fig. 5. Histone–DNA contacts enhance stability of the central region of nucleosomal DNA. (a) The number of endpoint bp detached as a function of time in an MD simulation of a nucleosome containing only the central 85-bp fragment of the Widom 601 DNA. The simulation was performed in 1 M $MgCl_2$; initial structure shown on the left. (b) The inner and outer regions of DNA in a fully assembled nucleosome. (c) Trajectory-average number of contacts that a histone core forms with the inner or the outer regions of the DNA per bp. A contact is defined as having a non-hydrogen protein atom within 4.5 Å of a non-hydrogen DNA atom. The bps detached from the histone core were not included in the calculation. Error bars represent standard deviations. The DNA sequence and electrolyte condition identified by label.

partially bound, and then (2) about one turn of DNA unbinds completely. This mechanism was then confirmed by inducing a partially bound state for nucleosomal DNA at six major sites where the minor groove faces toward the histone core (one shown in Fig. 4a), and then observing accelerated DNA unwrapping (Fig. 4b and c). Together, spontaneous and induced nucleosome unwrappings of nucleosomes featuring four DNA sequences strongly suggest that greater CG content corresponds to more stable nucleosomes. A recent MD study of poly-lysine peptide binding to DNA suggests that histone tails could bind to CG-rich DNA more tightly than to AT-rich DNA, which would make the sequence dependence of nucleosome unraveling reported in this study even more pronounced [75].

Our results suggest that different mechanisms may govern the unwrapping of outer and inner nucleosomal DNA. Outer stretches of DNA, far from the pseudo-dyad, may rapidly unwrap and rewrap from the histone core spontaneously, while chaperones may be required to extend unwrapping to more central DNA. The sensitivity of unwrapping to nucleosomal DNA CG content observed here may be enhanced when forces or torques are applied to the DNA endpoints. The mutation or chemical modification of specific highly conserved histone residues identified in this study to form important interactions with DNA could increase the rate of unwrapping or signal the initiation of transcription. Our study's observation of transient nucleosome unwrapping and rewrapping is consistent with models of nucleosome energetics based on genome-wide maps, which indicate that nucleosomes often exist in partially wrapped states in a biological setting [76,77], and the results of this investigation could be used in the future to contribute an additional term to such a model. Along with bioinformatics [8,78] and experimental [79–81] studies, our findings support the possibility of a mechanism whereby the initiation of transcription in yeast or plants is signaled by AT-rich segments of DNA that form less stable nucleosomes.

Materials and Methods

General simulation protocols

All-atom MD simulations were performed using the amber99SB-ILDN-PHI force field for proteins [82], the amber99-bsc0 variant for DNA [83], Young *et al.* [84] parameters for NaCl, the TIP3P water model [85], custom parameterization of Mg^{2+} ions [64], and the CUFIX corrections for non-bonded interactions between charged groups [86]. Periodic boundary

conditions were employed in all simulations, and long-range electrostatics were calculated using the Particle Mesh Ewald method [87] over a 1.6-Å spaced grid. Non-bonded Coulomb and Lennard–Jones interactions were truncated at 12 Å, and the non-bonded list was updated every 10 steps with the Verlet cutoff scheme [88]. Covalent bonds to hydrogen in water and in non-water molecules were constrained using SETTLE [89] and LINCS [90] algorithms, respectively. All minimization, structural relaxation, and initial unrestrained equilibration simulations of at least 50 ns were performed using the gromacs 5.0.4 MD package [91], in the constant number of particles N, pressure P, and temperature T ensemble at 1.0 bar and 300 K maintained using the V-rescaled, modified Berendsen thermostat [92] with a 0.1-ps time constant and the Parrinello–Rahman barostat [93] with a relaxation time of 2.0 ps. The 2-μs production runs were performed in the NPT ensemble on the D. E. Shaw Research Anton2 supercomputer [60]. The simulations on Anton2 employed a set of parameters equivalent to those listed above, except for using the Nosé–Hoover thermostat [94,95], the Martyna–Tobias–Klein barostat [96], and the k-space Gaussian split Ewald method [97] to calculate the electrostatic interactions.

All-atom models of nucleosome systems

A crystal structure of the canonical H3 nucleosome containing the Widom 601 [4] nucleosomal DNA (PDB ID: 3LZ0 [57]) served as the basis for all our structural models. The structure contained a protein core made up of eight histone proteins—two copies of histones H2A, H2B, H3, H4, and a 145-bp DNA fragment super-helically wrapped around the protein core. The protein model contained residues 16–118 for both copies of H2A, 29–121 for both copies of H2B, 39–134 for both copies of H3, and 25–102 for both copies of H4. The disordered N- and C-terminal tails of the core histones were not included in the model. The structural starting point for our models (PDB ID: 3LZ0 [57]) contains 145 bp of DNA, with a single bp at its center. Using a structure with an even number of bp would introduce a minor shift in the DNA's position. Overall, such a replacement would not lead to major changes, since 1-bp shifts were observed during spontaneous unwrapping and rewrapping (Supplementary Fig. S7).

Starting from the X-ray structure of the Widom 601 DNA nucleosome (PDB ID: 3LZ0 [57]), the *pdb2gmx* tool of gromacs was used to generate the computational model of the system. The protonation states of titratable residues were chosen to set the charge of Lys and Arg to $+1e$ (where e is the charge of a proton), Asp and Glu to $-1e$, and Gln and His to zero, the protonation state of all His residues was set to NE2. The resulting all-atom model was submerged in a cubic volume of water, producing a system of approximately 350,000 atoms, 150 Å on each side. The minimum distance between the periodic images of the nucleosomes was at least 30 Å. The all-atom model of the 601L nucleosome in physiological environment was produced by adding Na^+ and Cl^- ions to the system in the amount required to first neutralize the charge of the protein–DNA complex and then bring the ion concentration of the surrounding solvent to 0.15 M. The number of ions added to provide the desired concentrations c was determined using the expression $N_{ion} = 0.018\ c\ N_{water}$, where N_{ion} and N_{water} are the numbers of ions per species and water molecules, respectively.

Computational models of the 601L nucleosome in high ionic strength environments were produced by adding (1) Mg^{2+} and Cl^- ions to neutralize the nucleosome charge and bring the ion concentration to 1 M $MgCl_2$, and, separately, (2) Na^+ and Cl^- ions were introduced to neutralize the charge and reach an ionic concentration of 3 M NaCl. For simulations in magnesium, we chose to use the hydrated model of Mg^{2+} ions, where each Mg^{2+} ion forms a permanent cluster with six surrounding water molecules—magnesium hexahydrate [64]. This model was parametrized to reproduce the osmotic pressure of model compounds and was validated through simulations of DNA array systems [98]. The integrity of each Mg^{2+}-hexahydrate complex was maintained by applying harmonic potentials between the magnesium and water oxygen atoms; the spring constant of the potential k = 500,000 kJ mol^{-1} nm^{-2} and the equilibrium distance was 1.94 Å.

Upon assembly, the systems were minimized using the steepest descent method [99], until the maximum force on any atom was less than 166 pN. Absolute position restraints (k_{pos} = 1000 kJ mol^{-1} nm^{-2}) were applied during the minimization to all non-hydrogen atoms of the protein and DNA to maintain their crystallographic coordinates. The minimized systems were equilibrated in several steps (see Supplementary Table S4 and Fig. S1). Briefly, a network of pairwise harmonic restraints was applied within and between the DNA backbone and histone core, and gradually reduced to 0 over the course of 3.5 ns. The final configuration obtained at the end of the multi-step structural relaxation process was used for a ~2-μs production simulation, which was performed in the absence of any restraints, in the NPT ensemble at 1.0 bar and 300 K. The coordinates, velocities, and energies were saved every 2 ps for further analysis.

The same steps were repeated to generate the all-atom models of nucleosomes containing DNA of other, non-601L, nucleotide sequences. First, the nucleotide sequence of target DNA was compared to the 601 sequence of the DNA resolved in the X-ray structure. The base moieties of bps that did not match were modified to conform to the target sequence using the *psfgen* tool of VMD [100]; the coordinates of the DNA backbone were not altered. The resulting

conformations of newly generated bases were verified by computing the dihedral angle between the two atoms of the sugar backbone and the two of each base forming the glycosidic bond. The system featuring only the central 85-bp segment of Widom 601 DNA was built by removing 30 bp from each DNA terminus. The resulting structures were solvated; ions were added to bring the concentration of $MgCl_2$ to 1 M. The EN of restraints and Watson–Crick base-paring restraints were generated for each system individually; the structural relaxation simulations followed exactly same protocols as for the 601L system. Supplementary Table S1 lists the nucleotide sequences of DNA used to build all nucleosome systems considered in this work. The system containing only the 601L DNA was built by removing the histone proteins from the X-ray structure and adding 1 M $MgCl_2$ electrolyte. The production simulations of all systems were run for ~2 μs, except for the system featuring only the Widom 601L DNA (and no histone proteins), run for 0.3 μs, and simulations that forced the rupture of specific histone–DNA contacts (see Supplementary Methods 1, Table S3, and Fig. S8), which were run for 0.2 μs.

Supplementary data to this article can be found online at https://doi.org/10.1016/j.jmb.2018.11.013.

Acknowledgments

This work was supported by grants from NSF (PHY-1430124) and NIH (P41 GM104601). Supercomputer time was provided by XSEDE through allocation grant MCA05S028, the Blue Waters supercomputer at the University of Illinois, and Anton 2 allocation PSCA00052. Anton 2 computer time was provided by the Pittsburgh Supercomputing Center (PSC) through grant R01GM116961 from the National Institutes of Health. The Anton 2 machine at PSC was generously made available by D.E. Shaw Research. The authors thank Drs. Jun Song and Hu Jin for valuable discussions, and Drs. Jejoong Yoo and Christopher Maffeo for their assistance in preparing jobs to run on Anton 2.

Author Contributions: D.W. performed research. D.W. and A.A. designed the research project, analyzed data, and wrote the paper.

Conflict of Interest Statement: The authors declare no conflicts of interest.

Received 15 September 2018;
Received in revised form 26 October 2018;
Accepted 12 November 2018
Available online 20 November 2018

Keywords:
nucleosomes;
molecular dynamics;
DNA

Abbreviations used:
bp, base pair; MD, molecular dynamics; CG content, cytosine-guanine content.

References

[1] Y. Lorch, J.W. LaPointe, R.D. Kornberg, Nucleosomes inhibit the initiation of transcription but allow chain elongation with the displacement of histones, Cell 49 (1987) 203–210.
[2] K. Luger, A.W. Mader, R.K. Richmond, D.F. Sargent, T.J. Richmond, Crystal structure of the nucleosome core particle at 2.8 Å resolution, Nature 389 (1997) 251–260.
[3] C.A. Davey, D.F. Sargent, K. Luger, A.W. Maeder, T.J. Richmond, Solvent mediated interactions in the structure of the nucleosome core particle at 1.9 Å resolution, J. Mol. Biol. 319 (2002) 1097–1113.
[4] P.T. Lowary, J. Widom, New DNA sequence rules for high affinity binding to histone octamer and sequence-directed nucleosome positioning, J. Mol. Biol. 276 (1998) 19–42.
[5] A. Thåström, P. Lowary, H. Widlund, H. Cao, M. Kubista, J. Widom, Sequence motifs and free energies of selected natural and non-natural nucleosome positioning DNA sequences, J. Mol. Biol. 288 (1999) 213–229.
[6] G. Li, M. Levitus, C. Bustamante, J. Widom, Rapid spontaneous accessibility of nucleosomal DNA, Nat. Struct. Mol. Biol. 12 (2005) 46–53.
[7] T.T.M. Ngo, Q. Zhang, R. Zhou, J. Yodh, T. Ha, Asymmetric unwrapping of nucleosomes under tension directed by DNA local flexibility, Cell 160 (2015) 1135–1144.
[8] D. Tillo, T.R. Hughes, G + C content dominates intrinsic nucleosome occupancy, BMC Bioinf. 10 (2009) 1.
[9] T.J. Richmond, C.A. Davey, The structure of DNA in the nucleosome core, Nature 423 (2003) 145.
[10] J.D. Anderson, P.T. Lowary, J. Widom, Effects of histone acetylation on the equilibrium accessibility of nucleosomal DNA target sites, J. Mol. Biol. 307 (2001) 977–985.
[11] M. Tomschik, H. Zheng, K. van Holde, J. Zlatanova, S.H. Leuba, Fast, long-range, reversible conformational fluctuations in nucleosomes revealed by single-pair fluorescence resonance energy transfer, Proc. Natl. Acad. Sci. U. S. A. 102 (2005) 3278–3283.
[12] W. Koopmans, A. Brehm, C. Logie, T. Schmidt, J.V. Noort, Single-pair FRET microscopy reveals mononucleosome dynamics, J. Fluoresc. 17 (2007) 785–795.
[13] A. Gansen, K. Tóth, N. Schwarz, J. Langowski, Opposing roles of H3- and H4-acetylation in the regulation of nucleosome structurea FRET study, Nucleic Acids Res. 43 (2015) 1433–1443.
[14] A. Miyagi, T. Ando, Y.L. Lyubchenko, Dynamics of nucleosomes assessed with time-lapse high-speed atomic force microscopy, Biochemistry 50 (2011) 7901–7908.
[15] J.A. North, J.C. Shimko, S. Javaid, A.M. Mooney, M.A. Shoffner, S.D. Rose, et al., Regulation of the nucleosome unwrapping rate controls DNA accessibility, Nucleic Acids Res. 40 (2012) 10215–10227.
[16] Y. Chen, J.M. Tokuda, T. Topping, J.L. Sutton, S.P. Meisburger, S.A. Pabit, et al., Revealing transient structures of nucleosomes as DNA unwinds, Nucleic Acids Res. 42 (2014) 8767–8776.

[17] Y. Chen, J.M. Tokuda, T. Topping, S.P. Meisburger, S.A. Pabit, L.M. Gloss, et al., Asymmetric unwrapping of nucleosomal DNA propagates asymmetric opening and dissociation of the histone core, Proc. Natl. Acad. Sci. U. S. A. 114 (2017) 334–339.
[18] A.P. Bird, CpG-rich islands and the function of DNA methylation, Nature 321 (1986) 209–213.
[19] M. Gardiner-Garden, M. Frommer, CpG islands in vertebrate genomes, J. Mol. Biol. 196 (1987) 261–282.
[20] A.M. Deaton, A. Bird, CpG islands and the regulation of transcription, Genes Dev. 25 (2011) 1010–1022.
[21] E.Y. Chua, D. Vasudevan, G.E. Davey, B. Wu, C.A. Davey, The mechanics behind DNA sequence-dependent properties of the nucleosome, Nucleic Acids Res. 40 (2012) 6338–6352.
[22] V. Iyer, K. Struhl, Poly (dA: dT), a ubiquitous promoter element that stimulates transcription via its intrinsic DNA structure, EMBO J. 14 (1995) 2570–2579.
[23] M. Sawadogo, R.G. Roeder, Interaction of a gene-specific transcription factor with the adenovirus major late promoter upstream of the TATA box region, Cell 43 (1985) 165–175.
[24] K. Luger, M.L. Dechassa, D.J. Tremethick, New insights into nucleosome and chromatin structure: an ordered state or a disordered affair? Nat. Rev. Mol. Cell Biol. 13 (2012) 436–447.
[25] V. Böhm, A.R. Hieb, A.J. Andrews, A. Gansen, A. Rocker, K. Tóth, et al., Nucleosome accessibility governed by the dimer/tetramer interface, Nucleic Acids Res. 39 (2010) 3093–3102.
[26] H. Schiessel, J. Widom, R. Bruinsma, W. Gelbart, Polymer reptation and nucleosome repositioning, Phys. Rev. Lett. 86 (2001) 4414.
[27] G. Längst, P.B. Becker, Nucleosome remodeling: one mechanism, many phenomena? Biochim. Biophys. Acta Gene Struct. Expr. 1677 (2004) 58–63.
[28] T.T. Ngo, T. Ha, Nucleosomes undergo slow spontaneous gaping, Nucleic Acids Res. 43 (2015) 3964–3971.
[29] H. Kang, Y.-G. Yoon, D. Thirumalai, C. Hyeon, Confinement-induced glassy dynamics in a model for chromosome organization, Phys. Rev. Lett. 115 (2015) 198102.
[30] H. Kenzaki, S. Takada, Partial unwrapping and histone tail dynamics in nucleosome revealed by coarse-grained molecular simulations, PLoS Comput. Biol. 11 (2015), e1004443.
[31] J. Lequieu, A. Córdoba, D.C. Schwartz, J.J. de Pablo, Tension-dependent free energies of nucleosome unwrapping, ACS Cent. Sci. 2 (2016) 660–666.
[32] B. Zhang, W. Zheng, G.A. Papoian, P.G. Wolynes, Exploring the free energy landscape of nucleosomes, J. Am. Chem. Soc. 138 (2016) 8126–8133.
[33] M.D. Pierro, B. Zhang, E.L. Aiden, P.G. Wolynes, J.N. Onuchic, Transferable model for chromosome architecture, Proc. Natl. Acad. Sci. U. S. A. 113 (43) (2016) 12168–12173.
[34] N. Korolev, A.P. Lyubartsev, L. Nordenskiöld, A systematic analysis of nucleosome core particle and nucleosome–nucleosome stacking structure, Sci. Rep. 8 (2018) 1543.
[35] T.C. Bishop, Molecular dynamics simulations of a nucleosome and free DNA, J. Biomol. Struct. Dyn. 22 (2005) 673–685.
[36] C.K. Materese, A. Savelyev, G.A. Papoian, Counterion atmosphere and hydration patterns near a nucleosome core particle, J. Am. Chem. Soc. 131 (2009) 15005–15013.
[37] M. Biswas, K. Voltz, J.C. Smith, J. Langowski, Role of histone tails in structural stability of the nucleosome, PLoS Comput. Biol. 7 (2011), e1002279.
[38] R. Ettig, N. Kepper, R. Stehr, G. Wedemann, K. Rippe, Dissecting DNA–histone interactions in the nucleosome by molecular dynamics simulations of DNA unwrapping, Biophys. J. 101 (2011) 1999–2008.
[39] H. Kono, K. Shirayama, Y. Arimura, H. Tachiwana, H. Kurumizaka, Two arginine residues suppress the flexibility of nucleosomal DNA in the canonical nucleosome core, PLoS One 10 (2015), e0120635.
[40] D. Winogradoff, H. Zhao, Y. Dalal, G.A. Papoian, Shearing of the CENP-A dimerization interface mediates plasticity in the octameric centromeric nucleosome, Sci. Rep. 5 (2015) 17038.
[41] R. Collepardo-Guevara, G. Portella, M. Vendruscolo, D. Frenkel, T. Schlick, M. Orozco, Chromatin unfolding by epigenetic modifications explained by dramatic impairment of internucleosome interactions: a multiscale computational study, J. Am. Chem. Soc. 137 (2015) 10205–10215.
[42] S. Bowerman, J. Wereszczynski, Effects of macroH2A and H2A. Z on nucleosome dynamics as elucidated by molecular dynamics simulations, Biophys. J. 110 (2016) 327–337.
[43] A.K. Shaytan, G.A. Armeev, A. Goncearenco, V.B. Zhurkin, D. Landsman, A.R. Panchenko, Coupling between histone conformations and DNA geometry in nucleosomes on a microsecond timescale: atomistic insights into nucleosome functions, J. Mol. Biol. 428 (2016) 221–237.
[44] M. Pasi, R. Lavery, Structure and dynamics of DNA loops on nucleosomes studied with atomistic, microsecond-scale molecular dynamics, Nucleic Acids Res. 44 (2016) 5450–5456.
[45] J. Lequieu, D.C. Schwartz, J.J. de Pablo, In silico evidence for sequence-dependent nucleosome sliding, Proc. Natl. Acad. Sci. U. S. A. 114 (44) (2017) E9197–E9205.
[46] T. Niina, G.B. Brandani, C. Tan, S. Takada, Sequence-dependent nucleosome sliding in rotation-coupled and uncoupled modes revealed by molecular simulations, PLoS Comput. Biol. 13 (2017), e1005880.
[47] C. Maffeo, J. Yoo, J. Comer, D.B. Wells, B. Luan, A. Aksimentiev, Close encounters with DNA, J. Phys. Condens. Matter 26 (2014), 413101.
[48] D.A. Potoyan, G.A. Papoian, Energy landscape analyses of disordered histone tails reveal special organization of their conformational dynamics, J. Am. Chem. Soc. 133 (2011) 7405–7415.
[49] D.A. Potoyan, G.A. Papoian, Regulation of the H4 tail binding and folding landscapes via Lys-16 acetylation, Proc. Natl. Acad. Sci. U. S. A. 109 (2012) 17857–17862.
[50] D. Winogradoff, I. Echeverria, D.A. Potoyan, G.A. Papoian, The acetylation landscape of the H4 histone tail: disentangling the interplay between the specific and cumulative effects, J. Am. Chem. Soc. 137 (2015) 6245–6253.
[51] H. Zhao, D. Winogradoff, M. Bui, Y. Dalal, G.A. Papoian, Promiscuous histone mis-assembly is actively prevented by chaperones, J. Am. Chem. Soc. 138 (2016) 13207–13218.
[52] S. Sharma, F. Ding, N.V. Dokholyan, Multiscale modeling of nucleosome dynamics, Biophys. J. 92 (2007) 1457–1470.
[53] K. Voltz, J. Trylska, N. Calimet, J.C. Smith, J. Langowski, Unwrapping of nucleosomal DNA ends: a multiscale molecular dynamics study, Biophys. J. 102 (2012) 849–858.
[54] J. Culkin, L. De Bruin, M. Tompitak, R. Phillips, H. Schiessel, The role of DNA sequence in nucleosome breathing, Eur. Phys. J. E 40 (2017) 106.
[55] J.S. Mitchell, J. Glowacki, A.E. Grandchamp, R.S. Manning, J.H. Maddocks, Sequence-dependent persistence lengths of DNA, J. Chem. Theory Comput. 13 (2017) 1539–1555.

[56] J.A. Nash, A. Singh, N.K. Li, Y.G. Yingling, Characterization of nucleic acid compaction with histone-mimic nanoparticles through all-atom molecular dynamics, ACS Nano 9 (2015) 12374–12382.
[57] D. Vasudevan, E.Y. Chua, C.A. Davey, Crystal structures of nucleosome core particles containing the '601' strong positioning sequence, J. Mol. Biol. 403 (2010) 1–10.
[58] H. Ferreira, J. Somers, R. Webster, A. Flaus, T. Owen-Hughes, Histone tails and the H3 αN helix regulate nucleosome mobility and stability, Mol. Cell. Biol. 27 (2007) 4037–4048.
[59] L. Bintu, T. Ishibashi, M. Dangkulwanich, Y.-Y.Y. Wu, L. Lubkowska, M. Kashlev, et al., Nucleosomal elements that control the topography of the barrier to transcription, Cell 151 (2012) 738–749.
[60] D.E. Shaw, J.C. Chao, M.P. Eastwood, J. Gagliardo, J.P. Grossman, C.R. Ho, et al., Anton, a special-purpose machine for molecular dynamics simulation, Commun. ACM 51 (2008) 91.
[61] T.D. Yager, C.T. McMurray, K.V. Holde, Salt-induced release of DNA from nucleosome core particles, Biochemistry 28 (1989) 2271–2281.
[62] A. Gansen, A. Valeri, F. Hauger, S. Felekyan, S. Kalinin, K. Tóth, et al., Nucleosome disassembly intermediates characterized by single-molecule FRET, Proc. Natl. Acad. Sci. U. S. A. 106 (2009) 15308–15313.
[63] H.S. Tims, K. Gurunathan, M. Levitus, J. Widom, Dynamics of nucleosome invasion by DNA binding proteins, J. Mol. Biol. 411 (2011) 430–448.
[64] J. Yoo, A. Aksimentiev, Improved parametrization of Li^+, Na^+, K^+, and Mg^{2+} ions for all-atom molecular dynamics simulations of nucleic acid systems, J. Phys. Chem. Lett. 3 (2012) 45–50.
[65] K. Polach, J. Widom, Mechanism of protein access to specific DNA sequences in chromatin: a dynamic equilibrium model for gene regulation, J. Mol. Biol. 254 (1995) 130–149.
[66] R.T. Simpson, D.W. Stafford, Structural features of a phased nucleosome core particle, Proc. Natl. Acad. Sci. U. S. A. 80 (1983) 51–55.
[67] D. Rhodes, Nucleosome cores reconstituted from poly (dA–dT) and the octamer of histones, Nucleic Acids Res. 6 (1979) 1805–1816.
[68] R.T. Simpson, P. Künzler, Chromatin and core particles formed from the inner histones and synthetic polydeoxyribonucleotides of defined sequence, Nucleic Acids Res. 6 (1979) 1387–1415.
[69] G.B. Brandani, T. Niina, C. Tan, S. Takada, DNA sliding in nucleosomes via twist defect propagation revealed by molecular simulations, Nucleic Acids Res. 46 (2018) 2788–2801.
[70] C.G. Baumann, S.B. Smith, V.A. Bloomfield, C. Bustamante, Ionic effects on the elasticity of single DNA molecules, Proc. Natl. Acad. Sci. U. S. A. 94 (1997) 6185–6190.
[71] G.S. Manning, The persistence length of DNA is reached from the persistence length of its null isomer through an internal electrostatic stretching force, Biophys. J. 91 (2006) 3607–3616.
[72] L.E. McMillan, A.C. Martin, Automatically extracting functionally equivalent proteins from SwissProt, BMC Bioinf. 9 (2008) 418.
[73] M.A. Hall, A. Shundrovsky, L. Bai, R.M. Fulbright, J.T. Lis, M.D. Wang, High-resolution dynamic mapping of histone–DNA interactions in a nucleosome, Nat. Struct. Mol. Biol. 16 (2009) 124–129.
[74] I. Kulić, H. Schiessel, Chromatin dynamics: nucleosomes go mobile through twist defects, Phys. Rev. Lett. 91 (2003) 148103.
[75] H. Kang, J. Yoo, B.-K. Sohn, S.-W. Lee, H.S. Lee, W. Ma, et al., Sequence-dependent DNA condensation as a driving force of DNA phase separation, Nucleic Acids Res. (2018) https://doi.org/10.1093/nar/gky639 (Published online).
[76] G. Locke, D. Tolkunov, Z. Moqtaderi, K. Struhl, A.V. Morozov, High-throughput sequencing reveals a simple model of nucleosome energetics, Proc. Natl. Acad. Sci. U. S. A. 107 (2010) 20998–21003.
[77] R.V. Chereji, A.V. Morozov, Ubiquitous nucleosome crowding in the yeast genome, Proc. Natl. Acad. Sci. U. S. A. 111 (2014) 5236–5241.
[78] N. Kaplan, I.K. Moore, Y. Fondufe-Mittendorf, A.J. Gossett, D. Tillo, Y. Field, et al., The DNA-encoded nucleosome organization of a eukaryotic genome, Nature 458 (2009) 362–366.
[79] K. Struhl, Naturally occurring poly (dA–dT) sequences are upstream promoter elements for constitutive transcription in yeast, Proc. Natl. Acad. Sci. U. S. A. 82 (1985) 8419–8423.
[80] D.W. Russell, M. Smith, D. Cox, V.M. Williamson, E.T. Young, DNA sequences of two yeast promoter-up mutants, Nature 304 (1983) 652–654.
[81] G. Tjaden, G.M. Coruzzi, A novel AT-rich DNA binding protein that combines an HMG I-like DNA binding domain with a putative transcription domain, Plant Cell 6 (1994) 107–118.
[82] S. Lindström, H. Andersson-Svahn, Overview of single-cell analyses: microdevices and applications, Lab Chip 10 (2010) 3363–3372.
[83] A. Perez, I. Marchan, D. Svozil, J. Sponer, T.E. Cheatham, C.A. Laughton, et al., Refinement of the AMBER force field for nucleic acids: improving the description of α/γ conformers, Biophys. J. 92 (2007) 3817–3829.
[84] I.S. Joung, T.E. Cheatham, Determination of alkali and halide monovalent ion parameters for use in explicitly solvated biomolecular simulations, J. Phys. Chem. B 112 (2008) 9020–9041.
[85] W.L. Jorgensen, J. Chandrasekhar, J.D. Madura, R.W. Impey, M.L. Klein, Comparison of simple potential functions for simulating liquid water, J. Chem. Phys. 79 (1983) 926–935.
[86] J. Yoo, A. Aksimentiev, New tricks for old dogs: improving the accuracy of biomolecular force fields by pair-specific corrections to non-bonded interactions, Phys. Chem. Chem. Phys. 20 (2018) 8432–8449.
[87] T.A. Darden, D. York, L. Pedersen, Particle mesh Ewald: an $N\log(N)$ method for Ewald sums in large systems, J. Chem. Phys. 98 (1993) 10089–10092.
[88] S. Páll, B. Hess, A flexible algorithm for calculating pair interactions on SIMD architectures, Comput. Phys. Commun. 184 (2013) 2641–2650.
[89] S. Miyamoto, P.A. Kollman, SETTLE: an analytical version of the SHAKE and RATTLE algorithm for rigid water molecules, J. Comput. Chem. 13 (1992) 952–962.
[90] B. Hess, H. Bekker, H.J.C. Berendsen, J.G.E.M. Fraaije, LINCS: a linear constraint solver for molecular simulations, J. Comput. Chem. 18 (1997) 1463–1472.
[91] M.J. Abraham, T. Murtola, R. Schulz, S. Páll, J.C. Smith, B. Hess, et al., GROMACS: high performance molecular simulations through multi-level parallelism from laptops to supercomputers, SoftwareX 1 (2015) 19–25.
[92] G. Bussi, D. Donadio, M. Parrinello, Canonical sampling through velocity rescaling, J. Chem. Phys. 126 (2007) 014101.

[93] M. Parrinello, A. Rahman, Polymorphic transitions in single crystals: a new molecular dynamics method, J. Appl. Phys. 52 (1981) 7182–7190.
[94] S. Nosé, A unified formulation of the constant temperature molecular dynamics methods, J. Chem. Phys. 81 (1984) 511–519.
[95] W.G. Hoover, Canonical dynamics: equilibrium phase-space distributions, Phys. Rev. A 31 (1985) 1695–1697.
[96] G.J. Martyna, D.J. Tobias, M.L. Klein, Constant pressure molecular dynamics algorithms, J. Chem. Phys. 101 (1994) 4177–4189.
[97] Y. Shan, J.L. Klepeis, M.P. Eastwood, R.O. Dror, D.E. Shaw, Gaussian split Ewald: a fast Ewald mesh method for molecular simulation, J. Chem. Phys. 122 (2005) 054101.
[98] J. Yoo, A. Aksimentiev, Improved parameterization of amine–carboxylate and amine–phosphate interactions for molecular dynamics simulations using the CHARMM and AMBER force fields, J. Chem. Theory Comput. 12 (2016) 430–443.
[99] R. Fletcher, M.J. Powell, A rapidly convergent descent method for minimization, Comput. J. 6 (1963) 163–168.
[100] W. Humphrey, A. Dalke, K. Schulten, VMD: Visual molecular dynamics, J. Mol. Graph. 14 (1996) 33–38.